# Strong-coupling superconductivity in the kagome metal math xmlns="http://www.w3.org/1998/Math/MathML">msub>mi mathvariant="normal">CsV/mi>mn>3/mn>/msub>msub> mi mathvariant="normal">Sb/mi>mn>5/mn> /msub>/math> revealed by soft point-contact spectroscopy

Ming-chong He (何明冲), Hai Zi (子海), Hong-xing Zhan (詹红星), Yu-qing Zhao (赵宇清), Cong Ren (任聪), Xing-yuan Hou (侯兴元), Lei Shan (单磊), Qiang-hua Wang (王强华), Qiangwei Yin (殷蔷薇), Zhijun Tu (涂志俊), Chunsheng Gong (龚春生), Hechang Lei (雷和畅), Zhong-yi Lu (卢仲毅), Qi Wang (王琦), Yan-peng Qi (齐彦鹏), Gen-fu Chen (陈根富), and Peng Xiong

Phys. Rev. B **106**, 104510 — Published 16 September 2022

DOI: 10.1103/PhysRevB.106.104510

# Strong coupling superconductivity in kagome metal $CsV_3Sb_5$ revealed by soft point-contact spectroscopy

Ming-chong He(何明冲)[1], Hai Zi(子海)[1], Hong-xing Zhan(詹红星)[1], Yu-qing Zhao(赵宇清)[1], Cong Ren(任聪)[1†], Xing-yuan Hou(侯兴元)[2], Lei Shan(单磊)[2], Qiang-hua Wang(王强华)[3‡], Qiang-wei Yin(殷蔷薇)[4], Zhijun Tu(涂志俊)[4], Chunsheng Gong(龚春生)[4], He-chang Lei(雷和畅)[4], Zhong-yi Lu(卢仲毅)[4], Qi Wang(王琦)[5,6], Yan-peng Qi(齐彦鹏)[5,6], Gen-fu Chen(陈根富)[7], Peng Xiong[8]

[1] *School of Physics and Astronomy, Yunnan University, Kunming 650500, China*

[2] *Information Materials and Intelligent Sensing Laboratory of Anhui Province, Institutes of Physical Science and Information Technology, Anhui University, Hefei 230601, China*

[3] *School of Physics, Nanjing University, Nanjing 210093, China*

[4] *Department of Physics and Beijing Key Laboratory of Opto-electronic Functional Materials & Micro-nano Devices, Renmin University of China, Beijing 100872, China*

[5] *School of Physical Science and Technology, ShanghaiTech University, Shanghai 201210, China*

[6] *ShanghaiTech Laboratory for Topological Physics, ShanghaiTech University, Shanghai 201210, China*

[7] *Beijing National Laboratory for Condensed Matter Physics, Institute of Physics, CAS, Beijing 100190, China and*

[8] *Department of Physics, Florida State University, Tallahassee, Florida 32306 USA*

(Dated: August 4, 2022)

The nature of the superconducting state in kagome metals $AV_3Sb_5$ is a key issue in need of experimental clarification. Here, we report on a study of the superconducting order parameter in the kagome superconductor $CsV_3Sb_5$ through simultaneous "soft" point-contact spectroscopy and resistivity measurements **under both ambient and a hydrostatic pressure**. **Signatures of two-gap superconductivity are resolved in the soft point-contact spectra, accompanied by an asymmetric excess conductance above $T_c$.** Quantitative analysis based on two-dimensional Blonder-Tinkham-Klapwijk (BTK) model reveals an $(s+s)$-wave superconducting gap with $2\Delta_0/k_BT_c \simeq 7.2$, placing $CsV_3Sb_5$ in the strong-coupling regime. The strong-coupling two-gap feature indicates a high electronic density of states (DOS) and possible existence of flat band-driven multiple van Hove singularities (vHss) at the Fermi level. The presence of asymmetric excess spectral conductance above $T_c$ hints at a modest electronic correlation in $CsV_3Sb_5$. Under a hydrostatic pressure of 2.1 kbar, the nodeless multigap nature of the superconducting state remains, **whereas both the larger gap and the excess spectral conductance are greatly suppressed, accompanying with an enhanced $T_c$. An estimate of spectral-weighted gap ratio reveals a weakened coupling strength, indicative of a reduced total superconducting DOS upon pressure.** Our results point to key roles of both flatband associated vHss and electronic correlation on the onset of kagome superconductivity. **and shed some light on the interplay between charge-density-wave order and superconductivity in vanadium-based kagome superconductors**.

## I. INTRODUCTION

The kagome lattice, consisting of a two-dimensional lattice of corner-sharing triangles, has become a paradigmatic setting for exotic quantum phenomena of electronic matter. Indeed, depending on the electron filling, on-site repulsion, and nearest-neighbor Coulomb interaction, the ground state of a kagome lattice system can be a quantum spin liquid [1–3], charge bond order [4, 5], charge density wave (CDW) [6–8], or spin density wave [9]. Intriguingly, the recently discovered superconductivity in vanadium-based kagome metals, $AV_3Sb_5$ (A=K, Rb, Cs), adds a new physical dimension of electronic order to this novel system [10–12], making the family an ideal playground to explore the correlation among superconductivity, CDW, and nontrivial band topology [13–15].

Concerning the physical origin of superconductivity in kagome metals $AV_3Sb_5$, theoretical considerations have ruled out the possibility of conventional electron-phonon coupling mechanism [16, 17]. Despite the absence of long-range magnetic order or localized magnetic moments, possible existence of magnetic fluctuations [10, 18] **was invoked as a potential pathway to unconventional superconductivity with a strong-coupling sublattice interference mechanism** due to proximity to the flatband associated multiple van Hove singularities (vHss) at the Fermi level [17, 19–21]. On the experimental side, a distinct superconducting double-dome is found to coexist with an intriguing CDW state in the temperature ($T$)-pressure ($p$) phase diagrams of $AV_3Sb_5$, reminiscent of established unconventional superconductors (SCs) [22–24]. **Signatures of unconventional superconductivity such as spin-triplet pairing were reported in $K_{1-x}V_3Sb_5$-based Josephson junctions [25]. However, as for the specific gap structure and superconducting coupling strength, different experimental probes have produced disparate results.** Thermal conductivity mea-

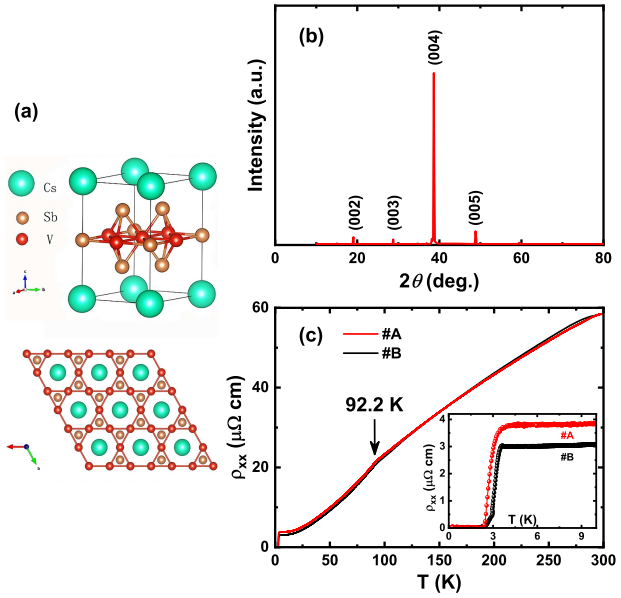


FIG. 1. (Color online) (a) Crystal structure of $CsV_3Sb_5$ and an illustration of a top view of the lattice. The vanadium sublattice forms a perfect kagome lattice. (b) X-ray diffraction pattern of a typical $CsV_3Sb_5$ single crystal with the corresponding Miller indices $(00l)$. (c) **Temperature dependence of resistivity $\rho_{xx}(T)$ for two pieces of $CsV_3Sb_5$ crystals**. The arrow marks the resistivity anomaly at the charge-density-wave transition. Inset: The resistivity in the superconducting transition regime.

surement appeared to suggest a nodal superconducting gap [26]. On the other hand, nuclear magnetic resonance experiments indicated a nodeless $s$-wave superconductivity competing with a unique CDW state [27, 28]. Penetration depth along with specific heat measurements collectively point to two nodeless gaps in weak-coupling limit in $CsV_3Sb_5$ [29], whereas low-$T$ scanning tunneling microspectroscopy (STM) appeared to show both nodal and nodeless sign-preserving gaps with multiple Fermi surfaces for the same material [30]. **In addition, the different experimental probes are known to have varied sensitivities to different aspects of the band and spatial structures (e.g., surface versus bulk). It is apparent that the strong coupling mechanism for kagome superconductivity has not been definitively established experimentally.**

In this work, we performed point contact spectroscopy (PCS) measurements on single crystalline $CsV_3Sb_5$ to investigate its state of superconducting pairing. From $T$-dependence of the zero-bias conductance and analyses of the differential conductance curves $G(V)$ with the modified two-dimensional (2D) Blonder-Tinkham-Klapwijk (BTK) model, we obtain the gap size and superconducting transition temperature $T_c^A$ on the same sample, resulting in reliable determination of the coupling strength for $CsV_3Sb_5$. **Our results highlight the importance of flatband associated van Hove singularities in pairing state of kagome superconductivity.**

## II. EXPERIMENTAL DETAILS

Single crystals of $CsV_3Sb_5$ were synthesized using the self-flux method, in two different laboratories whose crystals are labeled as #A and #B. The crystal structure of $CsV_3Sb_5$ is depicted in Fig. 1(a). Figure 1(b) displays the $x$-ray diffraction pattern of a $CsV_3Sb_5$ single crystal. Only $(00l)$ diffraction peaks can be detected, indicative of the good crystalline of the single crystal [31]. **Shown in the main panel of Fig. 1(c) is the $ab$-plane electrical resistivity $\rho_{xx}(T)$ in entire temperature range with the residual resistance ratio $RRR \equiv R(300K)/R(5K)$ of 16, and 19 for #A and #B, respectively; a resistivity anomaly around 92 K is apparent** and is ascribed to a CDW-like first-order phase transition. Meanwhile, $ab$-plane resistivity $\rho_{xx}$ in superconducting transition region, is displayed in the inset of Fig. 1(c), **showing bulk superconductivity with the onset superconductivity transition temperature $T_c^{onset}$ and the zero resistivity temperature $T_c^{zero}$ around 3.4 K and 2.5 K for both samples, respectively.**

Andreev reflection spectroscopy (ARS) has been utilized to probe the nature of the superconducting gap in many SCs, including the two-gap $MgB_2$ [32], topological superconductors $Cu_xBi_2Se_3$ [33], $PbTaSe_2$ [34, 35], and iron-based pnictides [36, 37]. The measurement of ARS can be implemented either with a metal-tip point contact or soft planar contact geometry. Specifically, the soft planar point-contacts have the advantage of avoiding inhomogeneous pressure or local strain effects induced by the metal tip, providing a pressureless spectroscopy measurement [38, 39]. **"Soft" planar contacts to the flat and shiny surface cleaved along the $c$-axis of $CsV_3Sb_5$ crystals were made using a thick silver paste bonding with platinum wires in a glove box. The typical size of these planar contacts is about 50-100 $\mu$m under a microscope. The hetero-contact is actually composed of many nano-contacts due to the nanocrystalline nature of the silver paint, analogous to the tip point-contact technique. The differential conductance spectra were recorded with the standard phase-sensitive lock-in technique in a quasi-four-terminal configuration, where an AC modulation was applied to the sample on top of a DC current bias. The contact resistance $R_J$ between the silver particles and $CsV_3Sb_5$ sample was usually in the range of 0.5-10 $\Omega$, typical values of a genuine point-contact between normal metals and superconductors.**

## III. RESULTS AND DISCUSSIONS

**Shown in the main panel of Fig. 2 (a) and (c) are a representative set of $G(V)$ curves at $T$ up to 10 K, far beyond the superconducting re-**

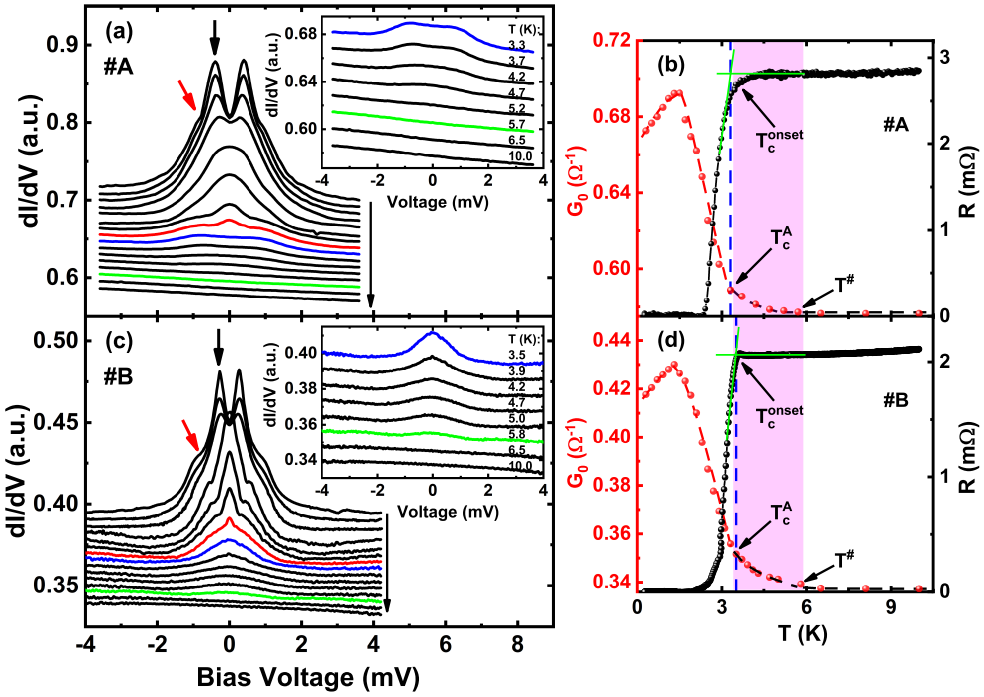


FIG. 2. (Color online) (a)(c) Raw data of soft point-contact conductance spectrum $G(V) \equiv dI/dV$ vs bias voltage $V$ at various $T$s from 0.3 K to 10.0 K for sample #A and #B, respectively. The $G(V)$ curves are vertically shifted for clarity except the one at the highest $T$. The insets are the enlarged view of SPCS at $T > T_c$. (b)(d) The corresponding zero bias conductance $G_0$ and resistance $R$ in the superconducting transition regime both as a function of $T$ for a comparison. **The dashed red and black lines in (b) and (d) are guided to the eye, and the vertical blue dashed lines in (b) and (d) represent the temperatures of 3.3 K and 3.5 K, respectively. The colored shadows in (b) and (d) marked the $G_0$-tail region between $T_c^A$ and $T^\#$.**

**sistive transition temperature $T_c^{onset} \simeq 3.4$ K for sample #A and #B, respectively. As shown, the $G(V)$ curves exhibit several common characteristics: At low-$T$s, $G(V)$ spectra display dips at zero-bias, and double shoulders at around 0.43 mV and double kinks around 1.0 mV, as marked by the black and red arrows, respectively. The double-shoulder and double-kink features are considered tell-tale signatures of** two-band superconductivity [38, 40]. Moreover, a dip, instead of a sharp peak at zero bias, excludes the possibility of a nodal gap in $CsV_3Sb_5$.

With increasing $T$, **an unexpected feature becomes apparent in these $G(V)$ curves when the overall magnitude of the Andreev conductance is gradually suppressed: As $T$ approaches the onset of the superconducting transition $T_c^{onset} \simeq 3.4$ K, the Andreev spectrum does not immediately reach bias-independent unity. Instead, as shown in the inset of Fig. 2(a), at 3.3 K, significant spectral conductance remains below about 1.0 mV with approximately 6% of Andreev intensity remaining at zero-bias (blue curve). The excess $G(V)$ gradually decreases, becoming essentially featureless at $T^\# \simeq 5.7$ K (green curve). With further increase of $T$, the $G(V)$ spectrum evolves into a $T$-independent, antisymmetric linear curve with a slight slope.** The excess conductance spectral in the high $T$ range manifests itself as an enhancement of the zero-bias conductance $G_0$ above the normal-state $G_N$. As shown in Fig. 2(b), $G_0$ shows a "tail" with a clear inflection point at $T_c^A$, the gap opening/closing temperature. Here, for sample #A, $T_c^A \simeq 3.3$ K almost coincides with $T_c^{onset}$, the upper superconducting resistive transition temperature, which rules out the existence of a pseudogap state in $CsV_3Sb_5$ [41]. Similar evolution of $G(V)$ in $T$, including the excess $G(V)$ and $G_0$ "tail" above $T_c^A$, is observed for sample #B with $T_c^A \simeq 3.5$ K and $T^\# \simeq 5.8$ K, as shown in Fig. 2(c) and (d). Very recently, the same behaviors of point-contact $G(V)$ spectra have been observed in both $CsV_3Sb_5$ and $KV_3Sb_5$ crystals [42].

**The observed excess spectra conductance in the normal state could be considered as fingerprints of the unconventional density of state (DOS) energy distribution in the vicinity of the Fermi level.** Theoretically, there is not presently a comprehensive model that fully accounts for the origin of the excess spectral conductance above $T_c$. Phenomenologically, for weakly correlated superconductors, such as $PbTaSe_2$ [34, 35], $PdBi_2$ [43], and (Y,Lu)$Ni_2B_2C$ [44], there is no excess $G(V)$ above $T_c$. In contrast, for strongly electron-

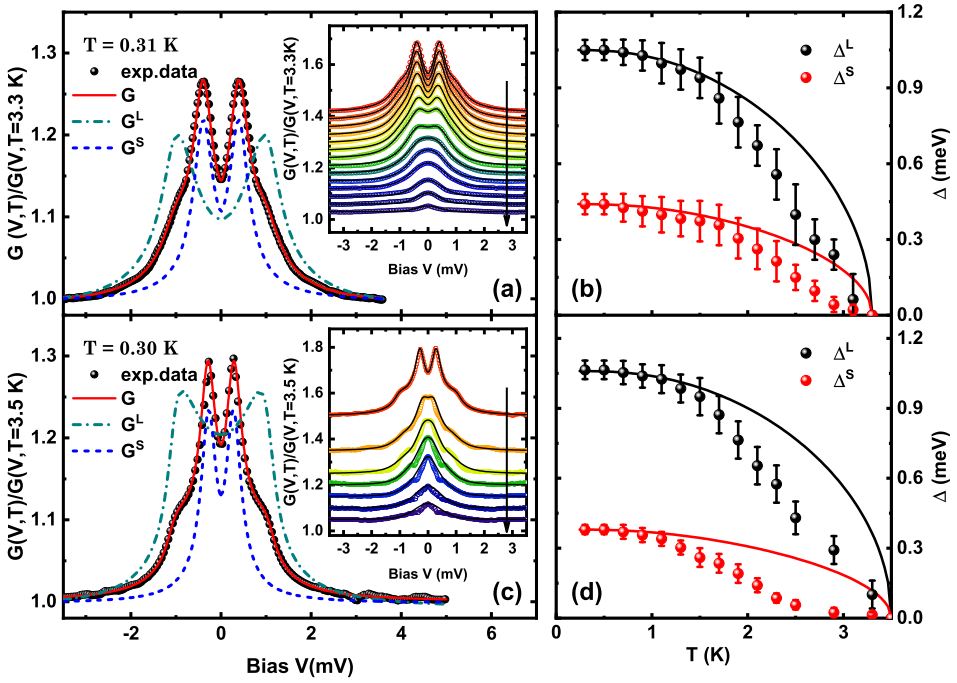


FIG. 3. (Color online) Normalized conductance spectrum $G(V)/G(V,T_c^A)$ for (a) #A and (c) #B at the lowest measurement $T$, and fittings based on the generalized 2D "BTK" model. The total conductance spectral $G(V)$ (solid red lines) is the summary of the partial conductance spectral $G^L$ and $G^S$ with the weight $\varpi$, i.e. $G(V) = \varpi G^L(V) + (1-\varpi)G^S(V)$. Insets: Temperature evolution of the normalized conductance curves **from** 0.3 **K to** 2.9 **K** and their fits by "2D" BTK model with the fixed $\varpi$. (b)(d) Temperature evolution of the extracted energy gaps $\Delta^L$ and $\Delta^S$ for samples #A and #B, respectively. The colored solid lines are the BCS $\Delta - T$ fitting lines.

correlated systems such as iron-pnictides [45] and heavy fermion superconductors [46, 47], excess $G(V)$ above $T_c$ is ubiquitous and is ascribed to electronic correlation effect [45, 46, 48]. We surmise that the presence of such broad excess $G(V)$ above $T_c$ and the resulting "tail" feature with positive curvature in $CsV_3Sb_5$ is an indicator of modest electron-electron correlations in such stoichiometric kagome metals.

To explicitly describe the variety of spectral behaviors observed and quantitatively extract the gap amplitude, we invoke a generalized "2D" Blonder-Tinkham-Klapwijk (BTK) model [49] with two $s$-wave conductance channels: $G(V) = \varpi G^L(V) + (1-\varpi)G^S(V)$, where $\varpi$ quantifies the relative spectral weight of the two channels. In the "2D" BTK model [50], the Andreev conductance spectrum $G(V)$ can be expressed with three parameters: a dimensionless parameter $Z$ which represents the interface transparency, an imaginary quasiparticle energy term $\Gamma$ (Dynes factor) which describes the spectral broadening, and the superconducting energy gap $\Delta$. As shown in the main panel of Fig. 3(a), the two-channel "2D" BTK model provides an excellent description of the normalized $G(V)$ at the lowest $T = 0.3$ K. The best fits yields $\Delta^L = 1.05$ meV, $\Gamma^L = 0.24$ meV, and $Z^L = 0.68$, for the large-gap channel, and $\Delta^S \simeq 0.45$ meV, $\Delta^S = 0.14$ meV, and $Z^S = 0.63$ for the small-gap channel. The spectral weight for the larger gap is around 27%, indicating a predominance of the small-gap channel. **The reliability of the analysis is further evidenced by similar results obtained from applying the same procedure to the #B Andreev junction.** The fittings are shown in the main panel of Fig. 3(c), which yield $\Delta^L = 1.06$ meV, $\Gamma^L = 0.12$ meV, $Z^L = 0.86$, and $\Delta^S = 0.38$ meV, $\Gamma^S = 0.12$ meV, $Z^S = 0.73$, and a spectral weight $\varpi \simeq 24\%$. **Here, the results, including the gap values and spectral weight, are highly consistent with those obtained from a similar soft PCS of $CsV_3Sb_5$ crystal [42].** Furthermore, the obtained gap values in $CsV_3Sb_5$ quantitatively agree with the prediction of a two-band electron-phonon coupling model, which sets boundaries for the two superconducting gaps [51], $\Delta^L > \Delta_{BCS} \simeq 0.52$ meV $> \Delta^S$, as observed in the canonical two-gap superconductor $MgB_2$ [52].

**Based on the best-fit parameters obtained above, we extend the analysis to all conductance spectra measured at temperatures below $T_c$.** As shown in the insets of Figs. 3(a) and 3(c), the two-gap "2D" BTK model provides good fits to all $G(V)$ curves. In all fittings, $\varpi$ is kept constant for each sample, while $\Gamma$ increases slightly with $T$ up to $T_c$. The resulting gaps $\Delta^L$ and $\Delta^S$ for #A and #B are plotted as functions of $T$, shown in Fig. 3(b) and 3(d), respectively. The obtained gaps can be approximated by an empirical BCS

formula: $\Delta(T) = \Delta_0 \tanh(\alpha\sqrt{T_c/T-1})$ where $\alpha$ is adjustable parameter [53]. **For sample #A, $\Delta_0^L = 1.05$ meV, $\Delta_0^S = 0.455$ meV. Here, $T_c$ as fitting parameters are equivalent to $T_c^A$ of #A and #B, as expected.**

We now discuss the implications of our results on the nature of superconductivity in the kagome superconductor $CsV_3Sb_5$. While the small gap of $\Delta^S \simeq 0.45$ meV coincides with one of those obtained by STM and $\mu$SR experiments [30, 54, 55], **the gap $\Delta^L \simeq 1.0$ meV is quite large in magnitude comparing with those reported from bulk nature measurements such as muon spin rotation/relaxation ($\mu$SR) [55] and specific heat experiments [29]. For example, $\mu$SR measurements of the magnetic penetration depth exhibits an $(s+s)$-wave gap symmetry with the larger gap of 0.57 meV and $T_c \simeq 2.5$ K [55]. One might argue that the larger gap of PCS measurement originates from surface state superconductivity as nontrivial topological surface states have been reported in these kagome compounds [11, 56], and the gap value for the topological surface superconductivity could be different from the bulk counterpart [57, 58]. However, in general, PCS is a bulk spectroscopic probe, and the probing depth is estimated to be about 2-3 $\xi$ ($\xi$ is the superconducting coherence length) into the sample surface [59]. Using $\mu_0 H_{c2}^{//ab} = \frac{\phi_0}{2\pi\xi_c^2}$, where $\mu_0 H_{c2}^{//ab}$ is the upper critical field ($\mu_0 H_{c2}^{//ab} \simeq 7.2$ Tesla for $CsV_3Sb_5$ [60]) and $\phi_0 = 2.07 \times 10^{-15}$ Wb the flux quantum, the probing length for ARS measurement is estimated to be about ~4-7 nm, confirming the bulk nature of the point-contact spectroscopy measurement. Moreover, the surface-sensitive STM experiment identified a larger superconducting gap of 0.56 meV [30], fully consistent with the bulk gap probed by $\mu$SR experiment. The consistency between the surface-sensitive and bulk gaps imposes a constraint on the existence of surface superconductivity of $CsV_3Sb_5$.**

Instead, we interpret the gap ratio $2\Delta_0^L/k_B T_c^A \simeq 7.2$ as an indicator of a strong coupling strength for $CsV_3Sb_5$. This value of coupling strength is much larger than those of typical two-gap superconductor $MgB_2$ ($\sim 4.16$) [32], topological superconductor $PbTaSe_2$ ($\sim$3.70) [34, 35], and typical CDW superconductors 2H-$NbSe_2$ ($\simeq 3.59$) and $TaS_2$ ($\simeq$3.85) [61, 62]; on the other hand, the coupling strength is close to those of iron-based superconductors, such as LiFeAs [63, 64], $KFe_2As_2$ ($\sim 7.2$) [65], in which there exists a van Hove singularity in the electronic density of states in the vicinity of the Fermi level $E_F$. In the framework of the conventional BCS theory, the superconducting gap is expressed as: $\Delta_{sc} \sim e^{-1/\lambda}$, where $\lambda$ is a product of $N(0)$, the DOS at the Fermi level, and $V_i$ the pairing interaction mediated by exchanging bosons [66]. In the scenario of electron-phonon coupling, a strong coupling strength implies a large DOS at $E_F$.

The high DOS at $E_F$ of $CsV_3Sb_5$ mainly arises from one or more flat band-associated vHss at the Fermi level. According to the first-principles electronic structure calculations [21, 67], the kagome bands can host two different types of vHss at the $M$-point in the Brillouin zone. Specifically, for $CsV_3Sb_5$, the calculations demonstrate that a van Hove singularity (vHs1) with the orbital content of V-$d_{x^2-y^2}$, $d_{z^2}$ and $d_{xy}$ in character is located at ~50 meV, and vHs2 with $d_{xz}$, $d_{yz}$ character is located at ~100 meV from $E_F$. Several angle-resolved photoemission spectroscopy (ARPES) studies have identified these twofold vHss near the Fermi level of $CsV_3Sb_5$, including both vHs1 and vHs2-type kagome bands. Among these vHss, the vHs2 is located closer to the Fermi level and is characterized by sharp Fermi surface nesting [68, 69]. As a consequence, the saddle points of vHs lead to a logarithmic divergence of DOS at $E_F$, thus suggesting the predominance of a high DOS for Cooper pairing in strong coupling strength. It is interesting to note that in magic-angle twisted bilayer graphene, a honeycomb lattice which resembles the kagome lattice, its superconductivity has been associated with the high DOS of its flat bands [70].

To gain further insight into the impact of the van Hove singularity on the superconductivity of $CsV_3Sb_5$, we performed $T$-dependent point-contact ARS combining with resistivity measurements on sample #A under a hydrostatic pressure of 2.1 kbar [34]. **As shown in the inset of Fig. 4(a), a $CsV_3Sb_5$/Ag point-contact junction together with a piece of $CsV_3Sb_5$ control sample was fed into a BeCu piston-cylinder cell (PCC) in which a quasi-hydrostatic pressure was generated by mechanically pressing Daphne 7373. The pressure values in PCC were determined from the change of superconducting transition temperature of Pb, $\Delta T_c^{Pb}$.** Shown in Fig. 4(a) is a set of conductance spectra at various $T$'s for the Andreev junction. **The conductance curves show a double-shoulder feature at 0.45 mV at low $T$s, which is nearly in agreement with that at ambient pressure. The most notable difference, however, is the kink feature in $G(V)$ is substantially weakened under such pressure. Moreover, concomitant with the suppression of the large gap feature, the broad excess $G(V)$ at $T > T_c^A$ fade away. Alternatively, the absence of excess $G(V)$ is evident in the $T$-dependence of the zero-bias conductance $G_0$, as shown in Fig. 4(b). Instead, under $p$, $G_0$ goes to a $T$-independent constant smoothly at an enhanced $T_c^A \simeq 4.2$ K, in accord with a similarly enhanced superconducting resistive transition temperature $T_c^{onset}$ by pressure.**

**We quantitatively analyze the measured Andreev reflection spectrum at $T = 0.28$ K by the aforementioned BTK fitting procedure. Notably, as shown in Fig. 4(c), the two $s$-wave gap model provides a noticeably better description of the**

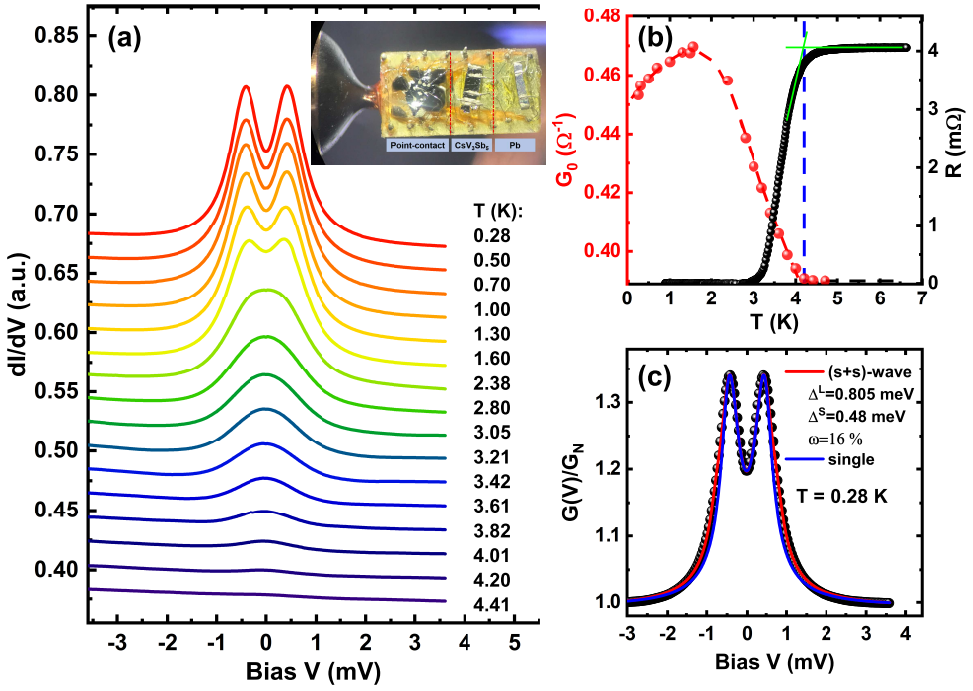


FIG. 4. (Color online) Conductance spectra and resistance of a bulk sample of #A both under a hydrostatic pressure. (a) Raw differential conductance curves $G(V)$ of a Ag/$CsV_3Sb_5$(#A) point-contact junction at various $T$s **under a quasi-hydrostatic pressure of 2.1 kbar**. The conductance spectrum $G(V)$ is vertically shifted for clarity except the one at the highest $T$. **The inset: the measuring configuration for pressure-dependent point-contact spectroscopy.** (b) The corresponding zero-bias conductance $G_0$ and resistance $R$ of a bulk sample #A in the superconducting transition regime both as a function of $T$ for a comparison. **The red and black dashed line are guided to the eye, with the vertical blue dashed lines representing the temperature of** 4.2 **K.** (c) The normalized conductance spectral $G(V)/G_N$ at the lowest $T$ and its fits to two $s$-wave (red solid curve). A single $s$-wave gap BTK fit is also plotted (blue solid curve) for a comparison.

**data than the one based on a single $s$-wave gap, indicating the persistence of the two nodeless superconducting gaps under the pressure. The best two-gap BTK-fit yields $\Delta^L = 0.81$ meV and $\Delta^S = 0.48$ meV, and a somewhat diminished spectral weight of $\varpi^L$=16% for the larger gap. Remarkably, the extracted small gap $\Delta^S$ almost remains essentially unchanged from that at ambient $p$, while both the amplitude and the spectral weight of the larger gap $\Delta^L$ are reduced upon applied $p$. Our observations seem to be consistent with those of a metal-tip locally pressurized $CsV_3Sb_5$ point-contact, in which case the larger gap and its spectral weight disappeared under a large local pressure or strain [42].** Band structure calculations show that under external $p$ both vHs1 and vHs2 experience a shift with respect to the Fermi level, manifesting as the saddle points moving linearly away from the Fermi level [67, 71, 72]. As the van Hove singularities located at the $M$ point move away from the Fermi level, it may induce a decrease in $N(0)$, and lead to the reduction of both the larger gap and its spectral weight contributing to superconductivity. On the other hand, the V-$d_{z^2}$-related van Hove singularity located at the Γ point is supposed to move closer to the Fermi level under pressure, accompanied by an increase in the $N(0)$ [72].

To elucidate the role of the DOS $N(0)$ at the Fermi level on the kagome superconductivity $CsV_3Sb_5$, we define a spectral-weighted superconducting gap $\Delta_{ave} = \varpi\Delta^L + (1-\varpi)\Delta^S$ **as a measure of the overall superconducting DOS at $E_F$ and examine its relation with the multi-gap superconductivity.** At $p$=2.1 kbar, $\Delta_{ave} \simeq 0.533$ meV, and $T_c^A \simeq 4.2$ K, leading to a weighted gap ratio $\frac{2\Delta_{ave}}{k_B T_c^A} \simeq 2.94$. **For a comparison, at ambient pressure $\Delta_{ave} \simeq 0.62$ meV with $T_c^A \simeq 3.3$ K, leading to a gap ratio of 4.36. The reduced coupling strength leads to a reduced total DOS for the superconducting state upon pressure. In the scenario of the electron-phonon strong coupling mechanism, the reduced total superconducting DOS at the Fermi-level can not account for the enhanced $T_c$ upon the hydrostatic pressure.**

In line with the argument that the excess $G(V)$ and the resulting positive curvature $G_0$-"tail" are the consequences of electronic correlation, our observation of the disappearance of excess $G(V)$ and $G_0$-"tail" under applied pressure **indicate the electronic correlation is effectively suppressed by the pressure, leading to**

**an enhancement of $T_c^{onset}$ and $T_c^A$.** Considering magnetic effects such as magnetic fluctuations and/or the V-3$d$ orbital order, Zhang *et al.* performed the DFT+$U$ calculations to examine the electronic correlation effect and the possible magnetism on the vanadium atoms [73]. **With a small $U$ value, a ferrimagnetic state with a nonzero net magnetic moment in the unit cell is found to be a more stable phase than those of the nonmagnetic state at ambient pressure. In this scenario, the hydrostatic pressure can be understood to effectively suppress the ferrimagnetism on the vanadium atoms and drive the system to a nonmagnetic state, and as a consequence restoring conventional superconductivity with an enhanced $T_c$. Therefore, although the kagome flat-band and their associated vHss have been considered an essential ingredient in the electronic structure of $CsV_3Sb_5$ relevant for the superconductivity, the role of the V-3$d$ inherent magnetism can not be disregarded [73], particularly for such magnetically frustrated kagome system.**

**Finally, we offer a general discussion on the interplay between the CDW order and superconductivity in $CsV_3Sb_5$ under the relatively low $p$. Under this pressure, the CDW transition occurs at $T_{CDW} \simeq 81.5$ K, as indicated by a resistivity anomaly [22, 23]. Increasing pressure leads to a suppression to the CDW, but no significant changes to the band structure in the normal state. In a Bilbro-McMillan partial gapping scenario, the CDW competes strongly with superconductivity at the Fermi surface [74]. Under this $p$, the CDW deformation strongly decreases the DOS at the Fermi energy by suppressing the van Hove singularities [72]. As a consequence, a decreasing $T_{CDW}$ indicates a reduced DOS due to the CDW order. As for the superconducting state, applying pressure decreases the total DOS for superconducting pairing. The situation contradicts the expected partial gapping scenario in the model of CDW-superconductivity competition, similar to the case of 2H-$NbSe_2$ in which the superconducting state is only weakly dependent on the pressure-modulated CDW state [75]. Future spectroscopy experiments should examine systematically the evolution of flat-band-associated vHss and the relation between superconducting and CDW orders, together with the precise understanding of the magnetism of the V-atoms under varying pressures.**

## IV. CONCLUSIONS

We have performed soft point-contact Andreev reflection spectroscopy combing with resistivity measurements on single crystals of the kagome superconductor $CsV_3Sb_5$, in order to ascertain its superconducting coupling strength (gap size $\Delta$ and $T_c$). The distinct soft PCS spectra at low temperatures evidence multigap superconductivity under ambient and low pressure. The observation of a pronounced large superconducting gap together with excess spectral conductance spectrum above $T_c$, and their suppression by a hydrostatic pressure, points to the importance of both a strong coupling mechanism and electron correlations for the kagome superconductivity in $CsV_3Sb_5$ at ambient pressure. Taken together, the results suggest that pairing in $CsV_3Sb_5$ is likely to be conventional multi-gap in nature, but is partially suppressed by the magnetism on the vanadium atoms.

**Acknowledgement:** Cong Ren expresses gratitude to Professor Hai-hu Wen for insightful discussions. This work is supported by the National Natural Science Foundation of China (Grant No. 11774303, 11574373, 12074002,11974246). C. R. thanks the financial support from the Joint Fund of Yunnan Provincial Science and Technology Department (Grant No. 2019FY003008). X. Y. Hou acknowledge financial support by the National Natural Science Foundation of China (Grant No. 11804379). H. C. Lei was supported by the National Key R&D Program of China (Grant No. 2018YFE0202600), and Beijing Natural Science Foundation (Grant No. Z200005). Y. Q. would like to acknowledge the National Key R&D Program of China (Grant No. 2018YFA0704300), and P. X. acknowledges financial support by National Science Foundation Grant No. DMR-1905843.

† cren@ynu.edu.cn

‡ qhwang@nju.edu.cn

[1] M. R. Norman, Rev. Mod. Phys. 88, 041002 (2016).
[2] Y. Shimizu, K. Miyagawa, K. Kanoda, M. Maesato, G. Saito, Phys. Rev. Lett. 91, 107001 (2003).
[3] M. P. Shores, E. A. Nytko, B. M. Bartlett, and D. G. Nocera, J. Am. Chem. Soc. 127, 13462 (2005).
[4] A. O'Brien, F. Pollmann, and P. Fulde, Phys. Rev. B 81, 235115 (2010).
[5] F. Pollmann, K. Roychowdhury, C. Hotta, and K. Penc, Phys. Rev. B 90, 035118 (2014).
[6] Wan-Sheng Wang, Zheng-Zhao Li, Yuan-Yuan Xiang, and Qiang-Hua Wang, Phys. Rev. B 87, 115135 (2013).
[7] S. V. Isakov, S. Wessel, R. G. Melko, K. Sengupta, and Y. B. Kim, Phys. Rev. Lett. 97, 147202 (2006).
[8] F. H. Yu, D. H. Ma, W. Z. Zhuo, S. Q. Liu, X. K. Wen, B. Lei, J. J. Ying, X. H. Chen, Nature Communications 12, 3645 (2021).
[9] Shun-Li Yu and Jian-Xin Li, Phys. Rev. B 85, 144402 (2012).
[10] B. R. Ortiz, L. C. Gomes, J. R. Morey, M. Winiarski, M. Bordelon, J. S. Mangum, I. W. H. Oswald,

J. A. Rodriguez-Rivera, J. R. Neilson, S. D. Wilson, E. Ertekin, T. M. McQueen, E. S. Toberer, Phys. Rev. Materials 3, 094407 (2019).
[11] B. R. Ortiz, S. M. L. Teicher, Y. Hu, J. L. Zuo, P. M. Sarte, E. C. Schueller, A. M. M. Abeykoon, M. J. Krogstad, S. Rosenkranz, R. Osbron, R. Seshadri, L. Balent, J. He, and S. D. Wilson, Phys. Rev. Lett. 125, 247002 (2020).
[12] E. M. Kenney, M. J. Graf, S. M. L. Teicher, R. Seshadri, and S. D. Wilson, Phys. Rev. Materials 5, 034801 (2021).
[13] Nana Shumiya, Md. Shafayat Hossain, Jia-Xin Yin, Yu-Xiao Jiang, Brenden R. Ortiz, Hongxiong Liu, Youguo Shi, Qiangwei Yin, Hechang Lei, Songtian S. Zhang, Guoqing Chang, Qi Zhang, Tyler A. Cochran, Daniel Multer, Maksim Litskevich, Zi-Jia Cheng, Xian P. Yang, Zurab Guguchia, Stephen D. Wilson, and M. Zahid Hasan, Phys. Rev. B 104, 035131 (2021).
[14] F. H. Yu, T. Wu, Z. Y. Wang, B. Lei, W. Z. Zhuo, J. J. Ying, and X. H. Chen, Phys. Rev. B 104, L041103 (2021).
[15] Shuo-Ying Yang, Yaojia Wang, Brenden R. Ortiz, Defa Liu, Jacob Gayles, Elena Derunova, Rafael Gonzalez-Hernandez, Libor Smejkal, Yulin Chen, Stuart S. P. Parkin, Stephen D. Wilson, Eric S. Toberer, Tyrel McQueen, and Mazhar N. Ali, Sci. Adv. 6 : eabb6003 (2020).
[16] Jianzhou Zhao, Weikang Wu, Yilin Wang, and Shengyuan A. Yang, Phys. Rev. B 103, L241117 (2021).
[17] Hengxin Tan, Yizhou Liu, Ziqiang Wang, and Binghai Yan, Phys. Rev. Lett. 127, 046401 (2021).
[18] E. M. Kenney, B. R. Ortiz, C. Wang, S. D. Wilson, and M. J. Graf, J. Phys.: Condens. Matter 33 235801 (2021).
[19] Maximilian L. Kiesel and Ronny Thomale, Phys. Rev. B 86, 121105(R) (2012).
[20] Lizardo H. C. M. Nunes and Cristiane Morais Smith, Phys. Rev. B 101, 224514 (2020).
[21] Xianxin Wu, Tilman Schwemmer, Tobias Müller, Armando Consiglio, Giorgio, Sangiovanni, Domenico Di Sante, Yasir Iqbal, Werner Hanke, Andreas P. Schnyder, M. Michael Denner, Mark H. Fischer, Titus Neupert, and Ronny Thomale, Phys. Rev. Lett. 127, 177001 (2021).
[22] K. Y. Chen, N. N. Wang, Q. W. Yin, Z. J. Tu, C. S. Gong, J. P. Sun, H. C. Lei, Y. Uwatoko, J. -G. Cheng, Phys. Rev. Lett. 126, 247001 (2021).
[23] Xu Chen, Xinhui Zhan, Xiaojun Wang, Jun Deng, Xiaobing Liu, Xin Chen, Jian-gang Guo, Xiaolong Chen, Chin. Phys. Lett. 38 057402 (2021).
[24] B. Q. Song, X. M. Kong, W. Xia, Q. W. Yin, C. P. Tu, C. C. Zhao, D. Z. Dai, K. Meng, Z. C. Tao, Z. J. Tu, C. S. Gong, H. C. Lei, Y. F. Guo, X. F. Yang, S. Y. Li, arXiv:2105.09248.
[25] Yaojia Wang, Shuo-Ying Yang, Pranava K. Sivakumar, Brenden R. Ortiz, Samuel M.L. Teicher, Heng Wu, Abhay K. Srivastava, Chirag Garg, Defa Liu, Stuart S. P. Parkin, Eric S. Toberer, Tyrel McQueen, Stephen D. Wilson, Mazhar N. Ali, arXiv:2012.05898.
[26] C. C. Zhao, L. S. Wang, W. Xia, Q. W. Yin, J. M. Ni, Y. Y. Huang, C. P. Tu, Z. C. Tao, Z. J. Tu, C. S. Gong, H. C. Lei, Y. F. Guo, X. F. Yang, S. Y. Li, arXiv:2102.08356.
[27] Chao Mu, Qiangwei Yin, Zhijun Tu, Chunsheng Gong, Hechang Lei, Zheng Li, and Jianlin Luo, Chin. Phys. Lett. 38 077402 (2021).
[28] J. Luo, Z. Zhao, Y. Z. Zhou, J. Yang, A. F. Fang, H. T. Yang, H. J. Gao, R. Zhou, and Guo-qing Zheng, npj Quantum Materials 7, 30 (2022).
[29] Weiyin Duan, Zhiyong Nie, Shuaishuai Luo, Fanghang Yu, Brenden R. Ortiz, Lichang Yin, Hang Su, Feng Du, An Wang, Ye Chen, Xin Lu, Jianjun Ying, Stephen D. Wilson, Xianhui Chen, Yu Song, and Huiqiu Yuan, Sci. China-Phys. Mech. Astron. 64, 107462 (2021),.
[30] Han-Shu Xu, Ya-Jun Yan, Ruotong Yin, Wei Xia, Shijie Fang, Ziyuan Chen, Yuanji Li, Wenqi Yang, Yanfeng Guo, Dong-Lai Feng, Phys. Rev. Lett. 127, 187004 (2021).
[31] Yang Fu, Ningning Zhao, Zheng Chen, Qiangwei Yin, Zhijun Tu, Chunsheng Gong, Chuanying Xi, Xiangde Zhu, Yuping Sun, Kai Liu, and Hechang Lei, Phys. Rev. Lett. 127, 207002 (2021).
[32] P. Szabó, P. Samuely, J. Kačmarčik, T. Klein, J. Marcus, D. Fruchart, S. Miragha, C. Marcenat, and A. G. M. Jansen, Phys. Rev. Lett. 87, 137005 (2001).
[33] Satoshi Sasaki, M. Kriener, Kouji Segawa, Keiji Yada, Yukio Tanaka, Masatoshi Sato, and Yoichi Ando, Phys. Rev. Lett. 107, 217001 (2011).
[34] Hai Zi, Ling-Xiao Zhao, Xing-Yuan Hou, Lei Shan, Zhian Ren, Gen-Fu Chen, and Cong Ren, Chin. Phys. Lett. 37 097403 (2020).
[35] Tian Le, Yue Sun, Hui-Ke Jin, Liqiang Che, Lichang Yin, Jie Li, G. M. Pang, C. Q. Xu, L. X. Zhao, S. Kittaka, T. Sakakibara, K. Machida, R. Sankar, H. Q. Yuan, G. F. Chen, Xiaofeng Xu, Shiyan Li, Yi Zhou, Xin Lu, Science Bulletin 65, 1349 (2020).
[36] T. Y. Chen, Z. Tesanovic, R. H. Liu, X. H. Chen, and C. L. Chien, Nature 453, 1224 (2008).
[37] D. Daghero, M. Tortello, G. A. Ummarino, and R. S. Gonnelli, Rep. Prog. Phys. 74 124509 (2011).
[38] R. S. Gonnelli, D. Daghero, G. A. Ummarino, V. A. Stepanov, J. Jun, S. M. Kazakov, and J. Karpinski, Phys. Rev. Lett. 89, 247004 (2002).
[39] Yurii Naidyuk, Oksana Kvitnitskaya, Dmytro Bashlakov, Saicharan Aswartham, Igor Morozov, Ivan Chernyavskii, Günter Fuchs, Stefan-Lüdwig Drechsler, Ruben Hühne, Kornelius Nielsch, Bernd Büchner, and Dmitriy Efremov, 2D Materials, 5, 045014 (2018).
[40] Z. Holanová, P. Szabó, P. Samuely, R. H. T. Wilke, S. L. Bud'ko, and P. C. Canfield, Phys. Rev. B 70, 064520 (2004).
[41] Hui Chen, Haitao Yang, Bin Hu, Zhen Zhao, Jie Yuan, Yuqing Xing, Guojian Qian, Zihao Huang, Geng Li, Yuhan Ye, Qiangwei Yin, Chunsheng Gong, Zhijun Tu, Hechang Lei, Shen Ma, Hua Zhang, Shunli Ni, Hengxin Tan, Chengmin Shen, Xiaoli Dong, Binghai Yan, Ziqiang Wang, Hong-Jun Gao, Nature 599, 222 (2021).
[42] Lichang Yin, Dongting Zhang, Chufan Chen, Ge Ye, Fanghang Yu, Brenden R. Ortiz, Shuaishuai Luo, Weiyin Duan, Hang Su, Jianjun Ying, Stephen D. Wilson, Xianhui Chen, Huiqiu Yuan, Yu Song, and Xin Lu, Phys. Rev. B 104, 174507 (2021).
[43] Liqiang Che, Tian Le, C. Q. Xu, X. Z. Xing, Zhixiang Shi, Xiaofeng Xu, and Xin Lu, Phys. Rev. B 94, 024519 (2016).
[44] X. Lu, W. K. Park, S. Yeo, K.-H. Oh, S.-I. Lee, and S. L. Bud'ko, P. C. Canfield, and L. H. Greene, Phys. Rev. B 83, 104519 (2011).
[45] D.Daghero1 and R.S. Gonnelli, Supercond. Sci. Technol. 23, 043001 (2010).

[46] W.K. Park, J. L. Sarrao, J. D. Thompson, and L. H. Greene, Phys. Rev. Lett. 100, 177001 (2008).

[47] G. Goll, H. v. Löhneysen, I. K. Yanson, L. Taillefer, Phys. Rev. Lett. 70, 2008 (1993).

[48] Mikael Fogelström, W. K. Park, L. H. Greene, G. Goll, and Matthias J. Graf, Phys. Rev. B 82, 014527 (2010).

[49] G. E. Blonder, M. Tinkham, and T. M. Klapwijk, Phys. Rev. B 25, 4515 (1982).

[50] S. Kashiwaya, Y. Tanaka, M. Koyanagi, and K. Kajimura, Phys. Rev. B 53, 2667 (1996).

[51] V. G. Kogan, C. Martin, and R. Prozorov, Phys. Rev. B 80, 014507 (2009).

[52] H. J. Choi, D. Roundy, H. Sun, M. L. Cohen, and S. G. Louie, Nature 418, 758 (2002).

[53] H. Padamsee, J. E Neighbor, and C. A. Shiffman, Jour. Low Temp. Phys. 12, 387 (1973).

[54] Zuowei Liang, Xingyuan Hou, Fan Zhang, Wanru Ma, Ping Wu, Zongyuan Zhang, Fanghang Yu, J.-J. Ying, Kun Jiang, Lei Shan, Zhenyu Wang, and X.-H. Chen, Phys. Rev. X 11, 031026 (2021).

[55] Ritu Gupta, Debarchan Das, Charles Hillis Mielke III, Zurab Guguchia, Toni Shiroka, Christopher Baines, Marek Bartkowiak, Hubertus Luetkens, Rustem Khasanov, Qiangwei Yin, Zhijun Tu, Chunsheng Gong, and Hechang Lei, npj Quantum Materials 7, 49 (2022)

[56] Yong Hu, Samuel M. L. Teicher, Brenden R. Ortiz, Yang Luo, Shuting Peng, Linwei Huai, J. Z. Ma, N. C. Plumb, Stephen D. Wilson, J.-F. He, and M. Shi, Science Bulletin 67, 495 (2022).

[57] Wenyao Liu, Lu Cao, Shiyu Zhu, Lingyuan Kong, Guangwei Wang, Michal Papaj, Peng Zhang, Ya-Bin Liu, Hui Chen, Geng Li, Fazhi Yang, Takeshi Kondo, Shixuan Du, Guang-Han Cao, Shik Shin, Liang Fu, Zhiping Yin, Hong-Jun Gao, Hong Ding, Nature Communications 11, 5688 (2020).

[58] S. Y. Guan, P. J. Chen, M. W. Chu, R. Sankar, F. Chou, H. T. Jeng, C. S. Chang, and T. M. Chuang, Sci. Adv. 2: e1600894 (2016).

[59] Yu. G. Naidyuk, I. K. Yanson, Point-contact spectroscopy, Springer Series in Solid-State Sciences, 2005.

[60] Shunli Ni, Sheng Ma, Yuhang Zhang, Jie Yuan, Haitao Yang, Zouyouwei Lu, Ningning Wang, Jianping Sun, Zhen Zhao, Dong Li, Shaobo Liu, Hua Zhang, Hui Chen, Kui Jin, Jinguang Cheng, Li Yu, Fang Zhou, Xiaoli Dong, Jiangping Hu, Hong-Jun Gao, and Zhongxian Zhao, Chin. Phys. Lett. 38, 057403(2021).

[61] Xing-Yuan Hou, Fan Zhang, Xin-Hai Tu, Ya-Dong Gu, Meng-Di Zhang, Jing Gong, Yu-Bing Tu, Bao-Tian Wang, Wen-Gang Lv, Hong-Ming Weng, Zhi-An Ren, Gen-Fu Chen, Xiang-De Zhu, Ning Hao, and Lei Shan, Phys. Rev. Lett. 124, 106403 (2020).

[62] J. A. Galvis, L. Chirolli, I. Guillamon, S. Vieira, E. Navarro-Moratalla, E. Coronado, H. Suderow, and F. Guinea, Phys. Rev. B 89, 224512 (2014).

[63] Torben Hänke, Steffen Sykora, Ronny Schlegel, Danny Baumann, Luminita Harnagea, Sabine Wurmehl, Maria Daghofer, Bernd Büchner, Jeroen van den Brink and Christian Hess, Phys. Rev. Lett. 108, 127001 (2012).

[64] S. V. Borisenko, V. B. Zabolotnyy, D. V. Evtushinsky, T. K. Kim, I. V. Morozov, A. N. Yaresko, A. A. Kordyuk, G. Behr, A. Vasiliev, R. Follath, and B. Büchner, Phys. Rev. Lett. 105, 067002 (2010).

[65] Delong Fang, Xun Shi, Zengyi Du, Pierre Richard, Huan Yang, X.X.Wu, Peng Zhang, Tian Qian, Xiaxin Ding, Zhenyu Wang, T. K. Kim, M. Hoesch, Aifeng Wang, Xianhui Chen, Jiangping Hu, Hong Ding, Hai-Hu Wen, Phys. Rev. B 92, 144513 (2015).

[66] M. Tinkham, Introduction to Superconductivity (second edition), McGraw-Hill Book Co., New York 2004.

[67] Harrison LaBollita and Antia S. Botana, Phys. Rev. B 104, 205129 (2021).

[68] Mingu Kang, Shiang Fang, Jeong-Kyu Kim, Brenden R. Ortiz, Sae Hee Ryu, Jimin Kim, Jonggyu Yoo, Giorgio Sangiovanni, Domenico Di Sante, Byeong-Gyu Park, Chris Jozwiak, Aaron Bostwick, Eli Rotenberg, Efthimios Kaxiras, Stephen D. Wilson, Jae-Hoon Park, Riccardo Comin, Nature Physics 18, 301 (2022).

[69] Kosuke Nakayama, Yongkai Li, Takemi Kato, Min Liu, Zhiwei Wang, Takashi Takahashi, Yugui Yao, and Takafumi Sato, Phys. Rev. B 104, L161112 (2021).

[70] Myungchul Oh, Kevin P. Nuckolls, Dillon Wong, Ryan L. Lee, Xiaomeng Liu, Kenji, Watanabe, Takashi Taniguchi, and Ali Yazdani, Nature 600, 240 (2021).

[71] Alexander A. Tsirlin, Pierre Fertey, Brenden R. Ortiz, Berina Klis, Valentino Merkl, Martin Dressel, Stephen D. Wilson, Ece Uykur, SciPost Phys. 12, 049 (2022).

[72] Jian-Guo Si, Wen-Jian Lu, Yu-Ping Sun, Peng-Fei Liu, and Bao-Tian Wang, Phys. Rev. B 105, 024517 (2022).

[73] Jian-Feng Zhang, Kai Liu, Zhong-Yi Lu, Phys. Rev. B 104, 195130 (2021).

[74] Griff Bilbro and W. L. McMillan, Phys. Rev. B 14, 1887 (1976).

[75] Yejun Feng, Jiyang Wang, R. Jaramillo, Jasper van Wezel, S. Haravifard, G. Srajer, Y. Liu, Z.-A. Xu, P. B. Littlewood, and T. F. Rosenbaum, Proc. Natl Acad. Sci. USA 109(19), 7224 (2012).